

Axial stresses with toroidal lens-to-mount interfaces

Paul R. Yoder, Jr.

Consultant in Optical Engineering
1220 Foxboro Drive, Norwalk, CT 06851

ABSTRACT

We extend previously published analytical techniques for analyzing axial stress developed within a lens or similar rotationally symmetric element clamped into a mount by a retainer to include toroidal opto-mechanical interfaces.

1. INTRODUCTION

The design of the glass-to-metal interfaces in optical instruments has rightfully received considerable attention in the literature since it is well known that improper mechanical loading can decenter optical elements, distort surface figure, cause birefringence or lead to physical damage in stressful environments. Delgado and Hallinan¹, Bayar² and Yoder^{3,4} have discussed various mounting arrangements from the analytical viewpoint. These authors and others such as Hopkins⁵ emphasized the advantages of contacting the optical element on its polished (generally spherical) surfaces. The traditional interfaces with such surfaces are the line contact "sharp corner", the tangent cone and the spherical seat as illustrated in Fig. 1. Stresses within the optical element due to axial preload imparted at assembly by tightening the retainer and subsequently modified by thermally induced dimensional changes can be estimated with the equations described in the above references. These can then be compared to tolerable limits.

In general, stress is reduced whenever the area of elastic body contact at the interface increases. This area is the smallest with line contact (Fig. 1A) and increases as the curvatures of the contacting surfaces become more nearly equal in magnitude. The largest area (and hence the lowest clamping stress) occurs when the surfaces exactly match (Fig. 1C). The tangential interface (Fig. 1B) is preferred by many instrument designers as it offers a reasonable compromise between fabrication complexity and performance. Although it works well with convex and plane surfaces, the tangent cone is incompatible with concave optical surfaces. An alternate configuration that approaches the performance of the tangential interface while circumventing this geometrical difficulty is the toroidal interface. This paper addresses the toroidal interface in some detail.

2. ANALYTICAL CONSIDERATIONS

Delgado and Hallinan¹ first explained how to apply standard mechanical engineering equations such as those from Rourke⁶ to typical interfaces between lenses and mounts. Fig. 2 shows their analogy to the interface between a "sharp corner" of radius $R_2 = D_2/2$ and a lens

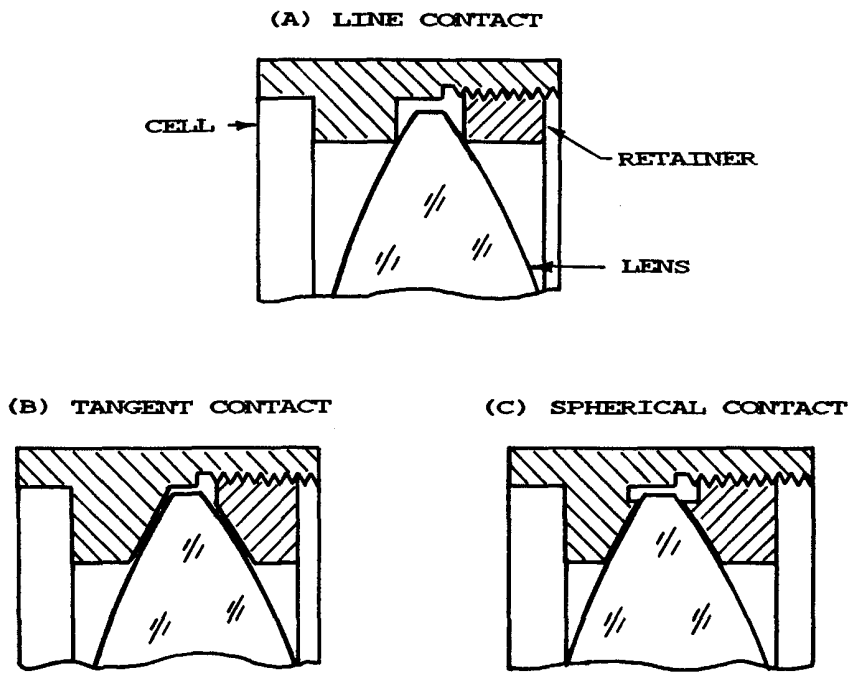


Fig. 1 Three traditional configurations for glass-to-metal interfaces in retaining-ring type clamped optical mounts.

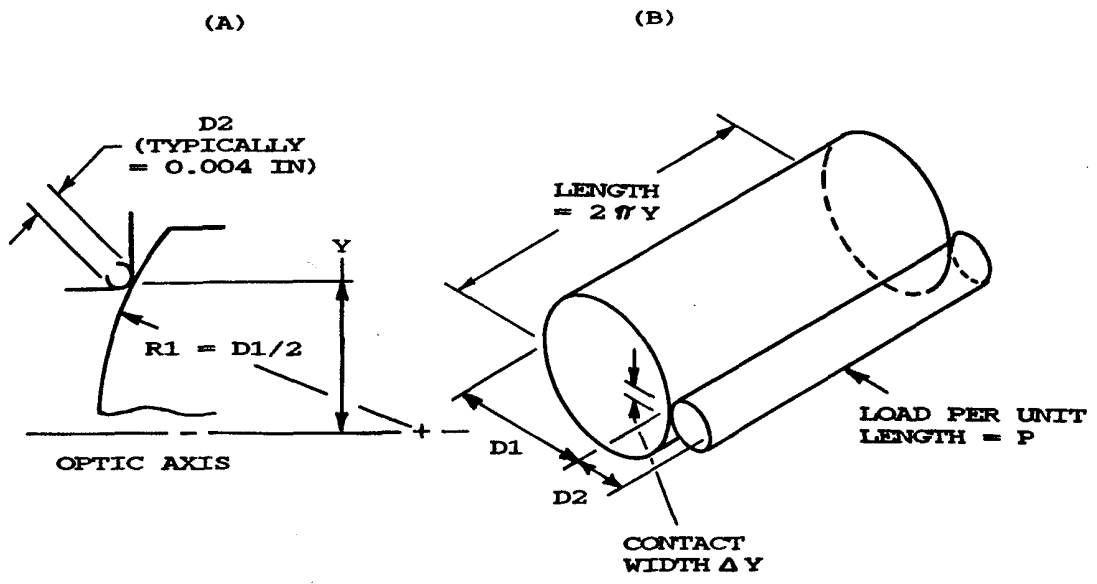


Fig. 2 Introduction of axial stress into a lens due to loading by a "sharp corner" interface. (A) geometric configuration; (B) analytical equivalent.

surface of radius $R_1 = D_1/2$. When forced together by an axially-directed load, the axial stress, S_A , is given by

$$S_A = 0.798 \left| \frac{P(D_1 + D_2)/D_1 D_2}{[(1 - \nu_G^2)/E_G] + [(1 - \nu_M^2)/E_M]} \right|^{1/2} \quad (1)$$

where: P = load per unit length of line contact
 D_1 = large cylinder diameter = twice lens radius
 D_2 = small cylinder diameter = twice corner radius
 ν_G = Poisson's ratio for the lens material
 ν_M = Poisson's ratio for the mount material
 E_G = Modulus of elasticity for the lens material
 E_M = Modulus of elasticity for the mount material.

In Ref. 1, a value of 0.1 mm (0.004 inch) for D_2 was taken to be typical of a machined "sharp edge". If this diameter were to be increased, the stress would be reduced. As a special case, if D_2 becomes infinite, we have the equivalent of a tangential cone interface. Eq. 1 would still apply, but the numerator within the brackets would reduce to P/D_1 .

The fact that D_2 is available as a design variable lead us to wonder how choice of this parameter affects the stress produced in a lens by a given preload P in an otherwise constant design. The interface is then called toroidal since the mounting edge resembles a "donut-shaped" toroid. With the minor constraint that the magnitude of D_2 be no larger than that of D_1 , such an edge can contact concave as well as convex or plane surfaces. This constraint does not apply to the latter cases. The following analysis addresses this issue.

3. THE TOROIDAL INTERFACE WITH A CONVEX SURFACE

Fig. 3 shows the upper half of a convex surface of radius R interfaced with toroidal surfaces of different relative radii $-R/2$ to $-R/32$. The tangent cone is the limiting toroidal radius considered here although the toroid could become concave and approach R_1 in magnitude. The angle of the surface normal relative to the axis is, of course, $\sin^{-1}(\text{contact height}/R)$. Using Eq. 1, we have computed the elastic stress developed in a 2 inch (50.8 mm) aperture BK7 glass lens clamped in an aluminum cell for surface radii R between 0.1 inch (2.54 mm) and infinity and toroid radii between 0.001 inch (0.025 mm) and 1000 inches (25,400 mm). The force per unit length, P , was also varied during this analysis. It was 1.0 lb/inch for all the cases depicted graphically in Fig. 4. For the shortest toroidal radius, the stress is essentially independent of surface radius and is about 43,400 lb/in². The usually accepted tolerances for optical glasses of 50,000 lb/in² maximum compressive stress and 500 lb/in² maximum stress to prevent excessive birefringence are indicated by the horizontal dashed lines. As the toroid radius is increased, each curve levels off and becomes asymptotic to a horizontal line at the stress characteristic of a tangential cone interface.

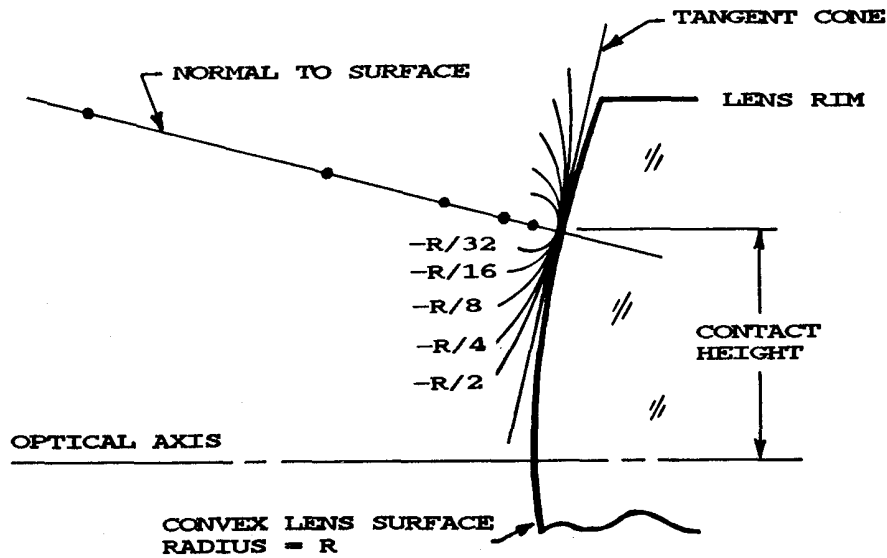


Fig. 3 Convex lens surface of radius R_1 interfaced with a tangent cone and convex toroidal surfaces of differing radii R_2 .

Fig. 5 shows cases identical to those of Fig. 4 except that the load P is decreased to 0.1 lb/in. Close examination of Eq. 1 reveals that the curves in Fig. 5 are identical to those of Fig. 4, but each point is displaced downward by the multiplying factor $(S_A)_2 / (S_A)_1 = (P_2 / P_1)^{1/2}$. In this case, this is $(0.1 / 1.0)^{1/2} = 0.316$.

An interesting observation results if we define the toroid radius as a fraction "k" of the lens surface radius, i.e., $D_2 = (k)(D_1)$, and substitute this into Eq. 1. The ratio of the stress at one value of "k" (k_2) to that at another value of "k" (k_1) for a constant D_1 is

$$\frac{S_2}{S_1} = \frac{((1 + k_2) / k_2)^{1/2}}{((1 + k_1) / k_1)^{1/2}} \quad (2)$$

Let S_1 represent the asymptotic (tangential) case wherein the toroidal radius becomes very large compared to the surface radius. Then k_1 approaches infinity and the denominator of Eq. 2 becomes unity. The ratio S_2 / S_1 varies with the assigned k_2 value as indicated in Table 1.

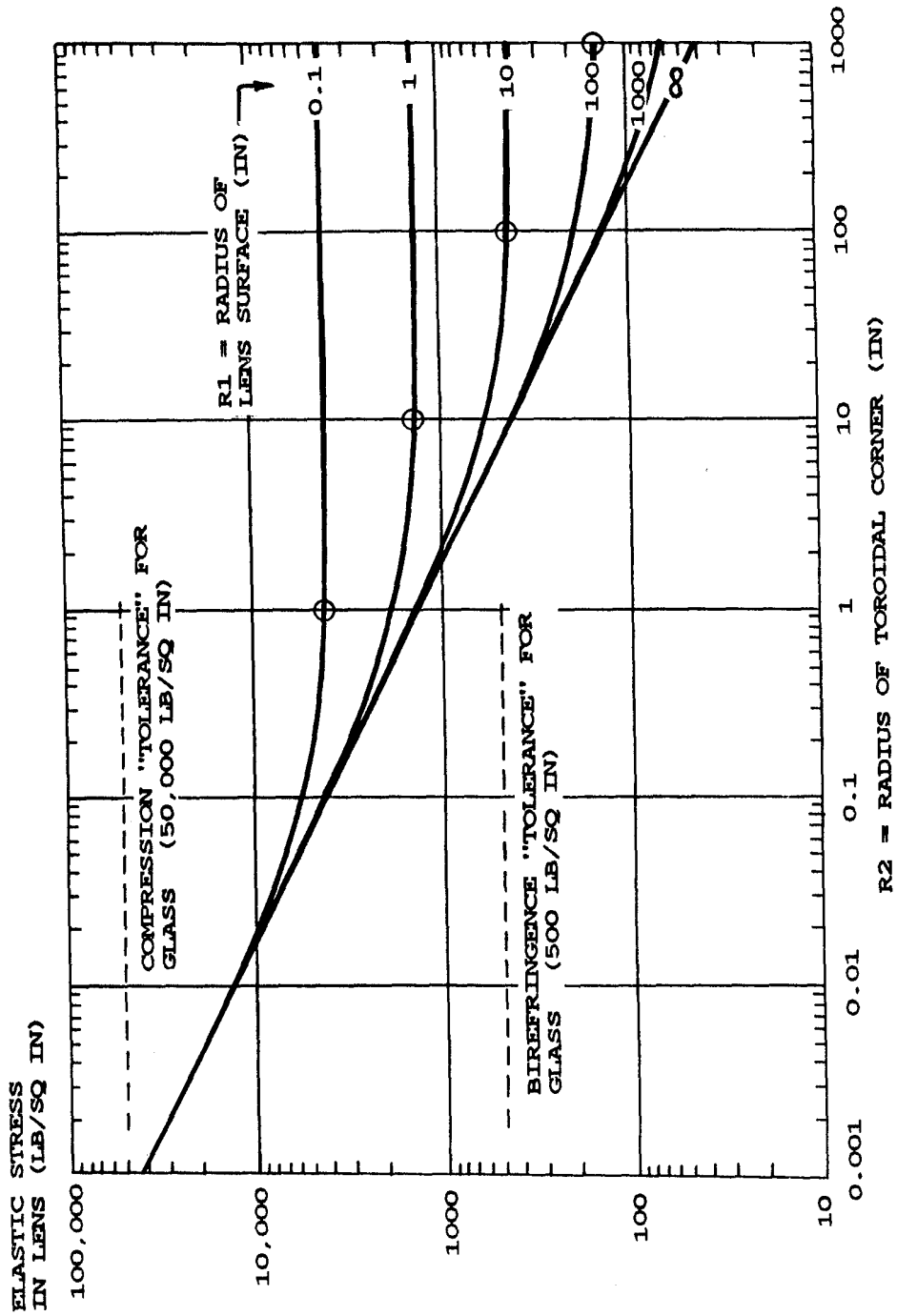


Fig. 4 Variation of axial stress with toroidal interface radius R_2 for different convex lens radii R_1 . BK7 lens diameter = 2 in, aluminum cell, linear load $P = 1.0$ lb/in.

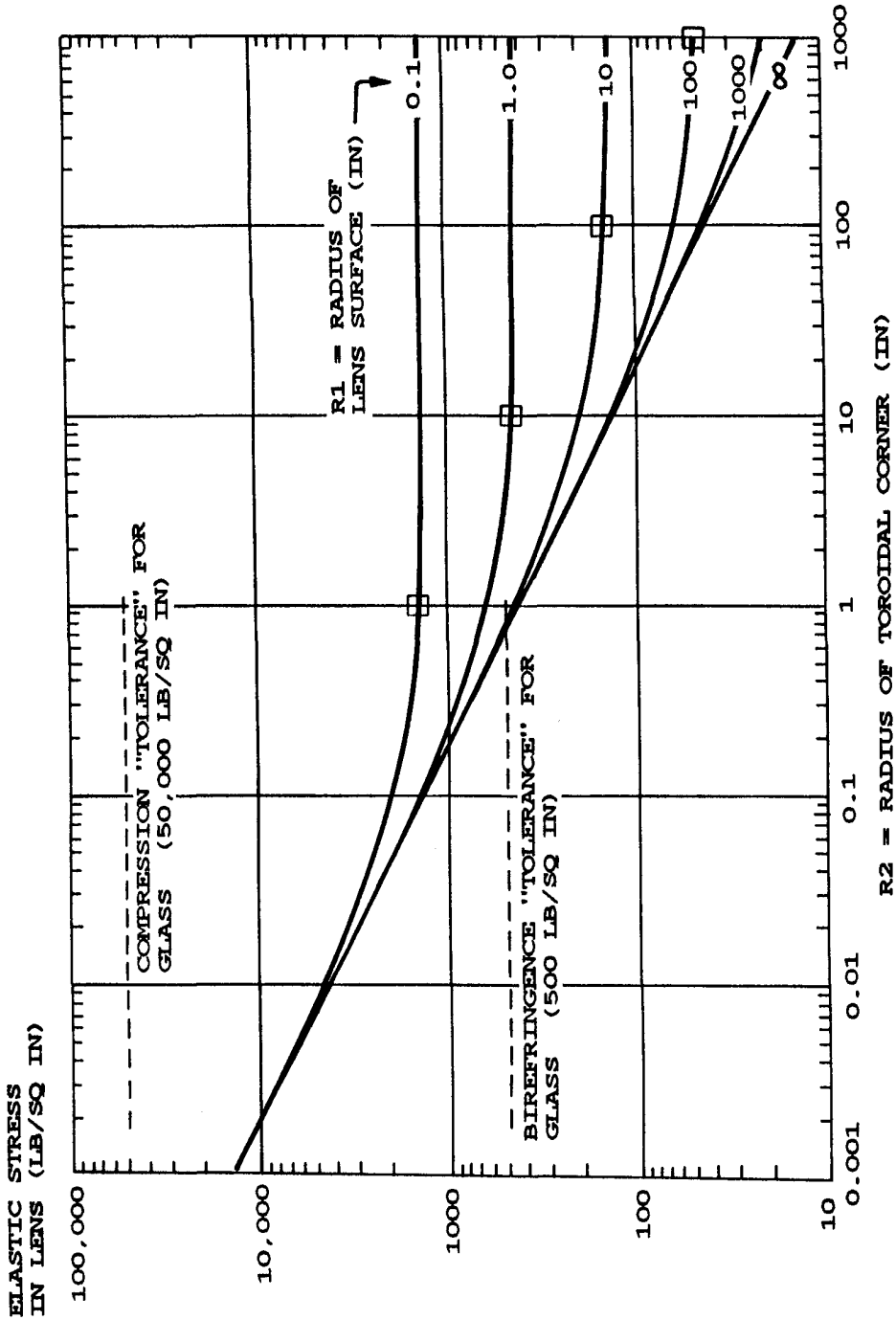


Fig. 5 Axial stress in the same lens as analyzed in Fig. 4, but with linear load $P = 0.1$ lb/in.

Table 1 - Ratio of Stress for Given "k₂" to Asymptotic Value

k ₂	S ₂ / S ₁	k ₂	S ₂ / S ₁
10 ⁻⁴	100.005	10 ⁰	1.414
10 ⁻³	31.639	10 ¹	1.049
10 ⁻²	10.049	10 ²	1.005
10 ⁻¹	3.317	10 ³	1.0005

We see that the departure of S₁ from the asymptotic value is always less than 5 percent when k₂ is at least 10. This leads us to the "rule of thumb" conclusion that essentially the same low stress condition as the tangential case results when the toroidal contact radius is 10 times the convex lens surface radius. This is true for all values of load "P" investigated here. The circles in Fig. 4 and the squares in Fig. 5 represent these conditions.

4. THE TOROIDAL INTERFACE WITH A CONCAVE SURFACE

Fig. 6 shows a series of toroidal mechanical interfaces with a concave surface of radius R. The toroid radius is again selected fractional multiples of R. The limiting case now is the matching

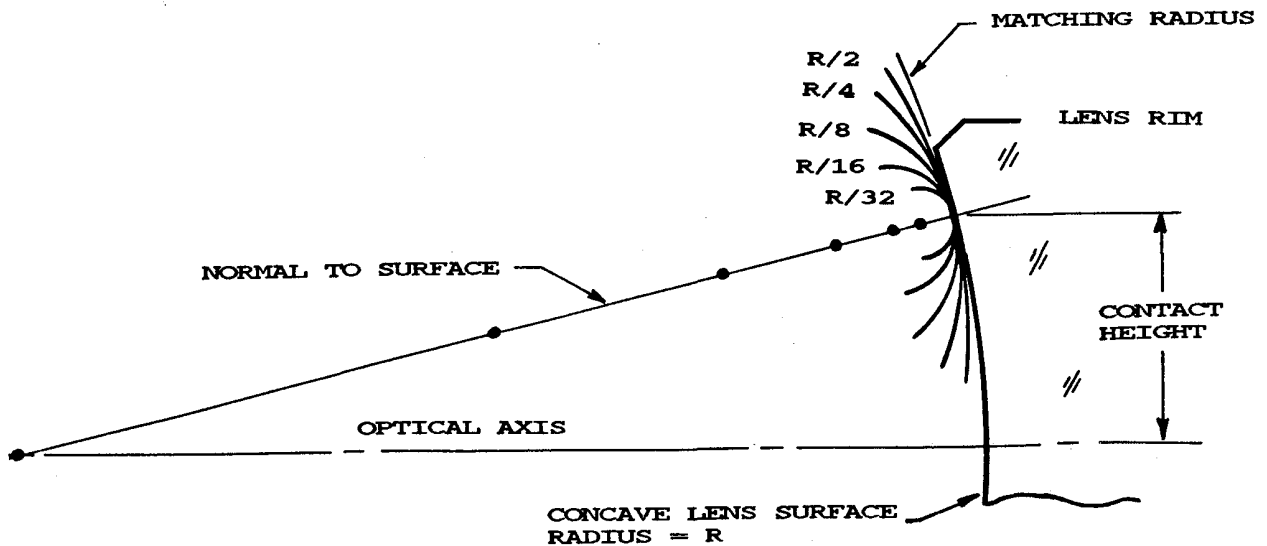


Fig. 6 Concave lens surface of radius R₁ interfaced with convex toroidal surfaces of differing radii R₂ including the matching radius.

radius. Again using Eq. 1, we computed the stress in the same BK7 lens/aluminum cell example considered above with $P = 1.0$ lb/inch and various values of D_1 and D_2 . The curves of Fig. 7 resulted. For very small toroid radii, the stress is once again high for all surface radii. As the toroid radius approaches the surface radius, the curves become asymptotic to vertical lines at $D_1 = D_2$ and the stress then drops rapidly to an insignificant value.

The points marked with triangles on each curve of Fig. 7 correspond to the stress values that would occur under the same load, P , on a convex surface of the same diameter and radius of curvature with a tangential interface. For 2 in diameter, BK7/aluminum designs, $S_A = 4327$ lb/in² at $R_1 = 0.1$ in, $S_A = 1368$ lb/in² at $R_1 = 1.0$ in, etc. Interestingly enough, these values always occur for a toroidal corner radius of 1/2 the surface radius. We thus can generalize that the same advantage of the tangential interface on the convex optical surface can thus be achieved with the corresponding concave surfaces by using a toroidal interface of at least 0.5 times the concave surface radius. Once again, with all other parameters constant, the stress at any one load value, P_2 can be derived from that at another value P_1 by multiplying by $(P_2/P_1)^{1/2}$.

Fig. 8 shows two of the many possible concepts for toroidal spacers as they might be used with various combinations of concave and/or convex surfaces. These interface configurations could also be applied to retaining rings and cell shoulders. The sketches are not to scale; dimensions are exaggerated for clarity of the concept. The configurations are generally compatible with conventional lathe turning methods or precision diamond machining. The locations of the toroid centers on the normals to the optical surfaces are indicated. If the quantitative guidelines discussed above were to be followed in actual designs, the corresponding radii would be considerably longer.

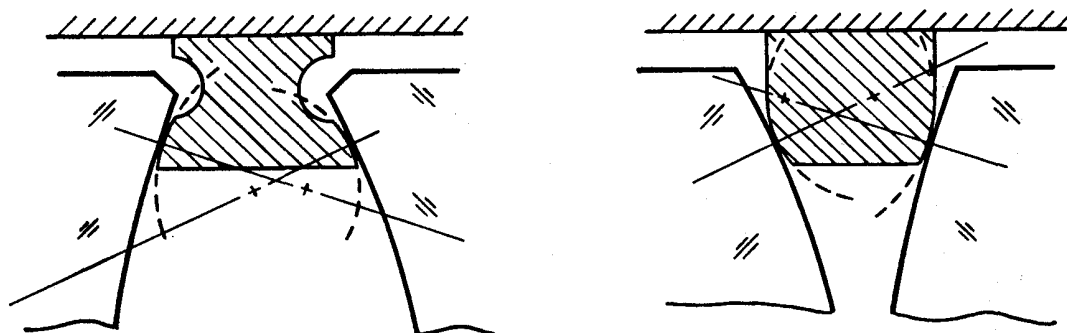


Fig. 8 Two suggested concepts for toroidal spacers to be used between concave and/or convex lens surfaces.

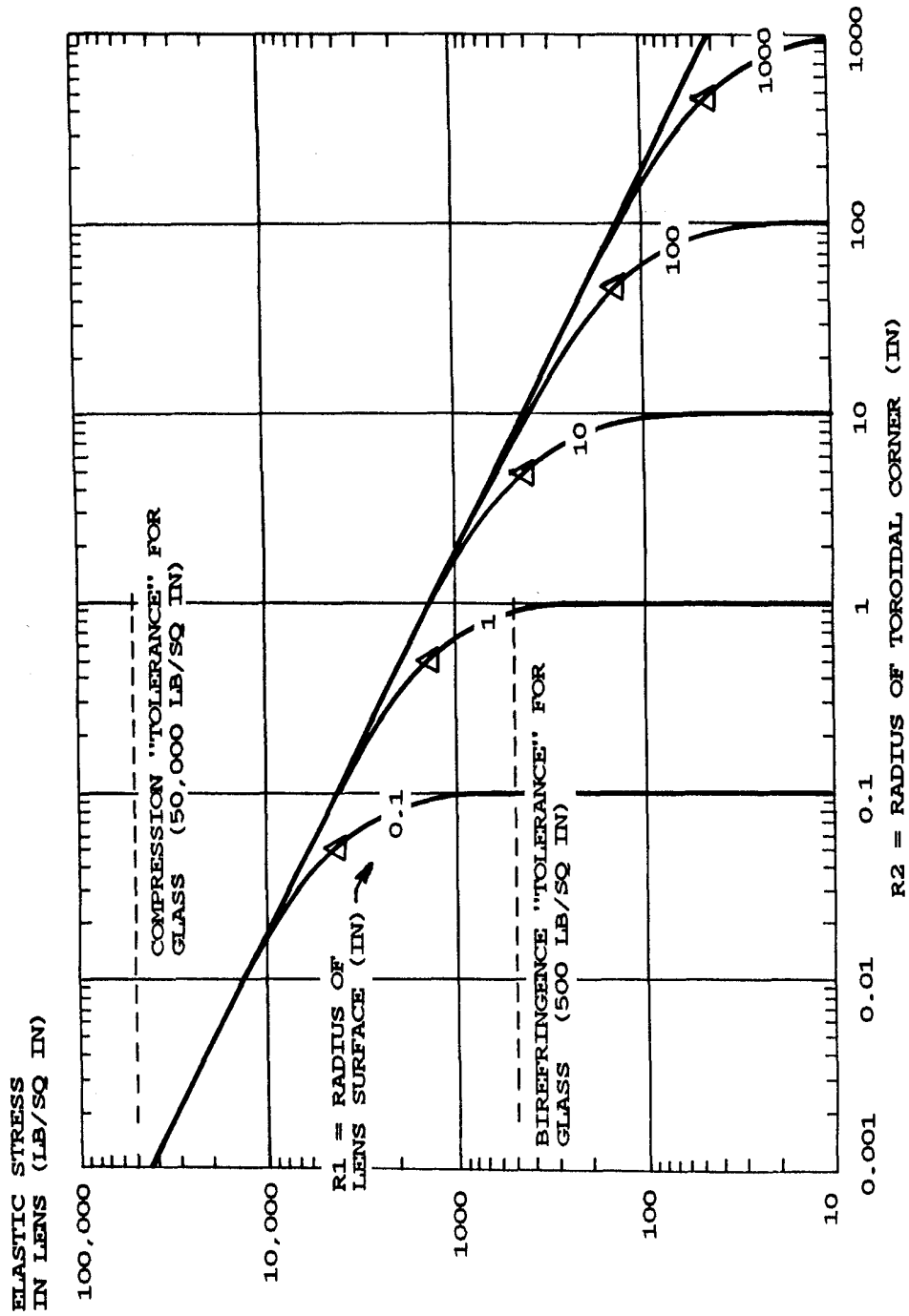


Fig. 7 Variation of axial stress with toroidal interface radius R_2 for different concave lens radii R_1 . BK7 lens diameter = 2 in, aluminum cell, linear load $P = 1.0$ lb/in.

Confirmation that the toroidal surface on a fabricated part actually has the profile radius specified on the drawing is not a simple matter. Templates give a rough check. Inspection with a stylus profilometer would allow a more precise evaluation. From Figs. 4 and 7, we see that both the stress magnitude and the sensitivity of the axial stress to toroidal radius error are smaller for longer radius toroids. This would lead us to design these to be as long as possible within the constraints of the particular application.

5. REFERENCES

1. Delgado, R.F. and Hallinan, M., "Mounting of Lens Elements", Opt. Eng. 14, S-11 (1975).
2. Bayar, M., "Lens Barrel Opto-Mechanical Design", Opt. Eng., 20, 181 (1981).
3. Yoder, P.R., Jr., "Lens Mounting Techniques", Proc. SPIE, 389, 2 (1983).
4. Yoder, P.R., Jr., Opto-Mechanical Systems Design, Marcel Dekker, New York (1986), pp 110-113.
5. Hopkins, R.E., "Some Thoughts on Lens Mounting", Opt. Eng., 15, 428 (1976).
6. Rourk, R.J., Formulas for Stress and Strain, 3rd edition, McGraw-Hill, New York (1954).